4. the cytoskeleton - network models

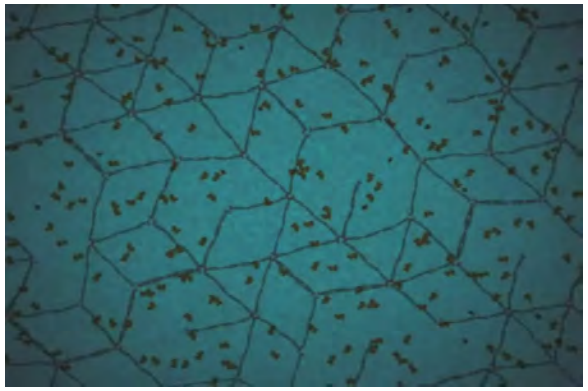

the inner life of a cell, viel & lue, harvard [2006]

day	date		topic
tue	apr	03	introduction I - cell biology
thu	apr	05	introduction II - cytoskeletal biology, stem cells
tue	apr	10	introduction III - structural mechanics
thu	apr	12	biopolymers I - energy, tension, bending
thu	apr	12	homework I - biopolymers, directed stem cell differentiation
tue	apr	17	biopolymers II - entropy, FJC and WLC model
thu	apr	19	biopolymers III - polymerization kinetics in amoeba
tue	apr	24	cytoskeletal mechanics I - fiber bundle model for filopodia
thu	apr	26	cytoskeletal mechanics II - network model for red blood cells
thu	apr	26	homework II - cytoskeleton, cell mechanics challenges
tue	may	01	cytoskeletal mechanics III - tensegrity model for generic eukaryotic cells
thu	may	03	biomembranes I - micropipette aspiration in white blood cells and cartilage cells
tue	may	08	biomembranes II - lipid bilayer, soap bubble, cell membrane
thu	may	10	biomembranes III - energy, tension, shear, bending
tue	may	15	mechanotransduction I - inter- and intracellular signaling, bone cells
tue	may	15	homework III - micropipette aspiration, final project
thu	may	17	summary and midterm preparation
tue	may	22	midterm
thu	may	24	mechanotransduction II - electrophysiology in nerve cells
tue	may	29	mechanotransduction III - excitation contraction in skeletal muscle and heart cells
thu	may	31	final projects I - oral presentations
tue	jun	05	final projects II - oral presentations
thu	jun	07	no class
fri	jun	08	final projects - written projects due

Homework II - The cytoskeleton

due Thu 05/03/12, 12:50pm, edu-128

You can drop off late homework in a box in front of Durand 217. Please mark clearly with date and time @drop off. We will take off 10 points for each 24 hours late.

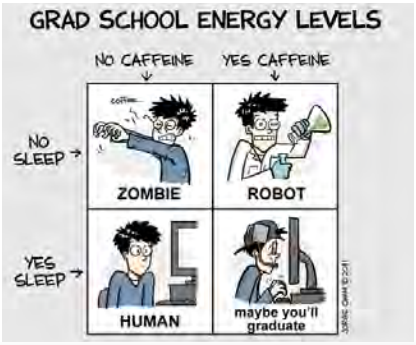

Problem 1 - Filament buckling

In class, we have discussed filament buckling of actin polymers. We have seen that the critical buckling force of filopodia

$$F_{\text{fil}} = \frac{\pi^2 EI}{[2\,L_{\text{fil}}]^2} = \frac{\pi^2 EI}{4\,L_{\text{fil}}^2}$$

can be increased by fascin which can create tightly crosslinked filament bundles.

- In class, we have assumed that there are about $n = 30$ actin filaments in one filopodium. Assume we do not know the exact number n. What is the minimum number of actin filaments to obtain a critical filopodia length of $L_{\text{fil}} = 5\mu m$ assuming that the actin filaments are (i) loosely assembled (4.2.9) and (ii) tightly crosslinked (4.2.12).
- How would the minimum number of required actin filaments n change if you assume a critical filopodia length of $L_{\text{fil}} = 2.5\mu m$?

Problem 2 - Forces on the cell membrane

To gain a better feeling for stresses that the cytoskeleton might induce on the cell membrane, this problem deals with the membrane pressure resulting from microtubules. Consider a generic spherical cell of radius 10μm with a tubulin heterodimer concentration of $C = n/V = 5\mu$M.

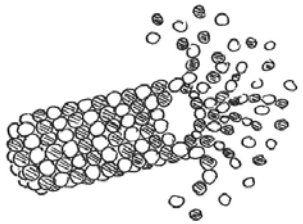

Figure. Microtubules are made up of rings of thirteen tubulin heterodimers which are 8 nm in diameter. The rings of tubulin heterodimers form a cylinder of thirteen protofilaments.

- Calculate the total length of microtubules that could be made from this amount of protein if each heterodimer is approximately 8 nm in diameter. Take into account that microtubules are made up of rings of thirteen tubulin heterodimers. Remember that 1μM = 1 μmol/liter and that 1 mol contains 6.02 $\cdot 10^{23}$ heterodimers.

Annals of Biomedical Engineering, Vol. 37, No. 5, May 2009 (© 2009) pp. 847–859
DOI: 10.1007/s10439-009-9661-x

Biomechanics: Cell Research and Applications for the Next Decade

DENNIS DISCHER,[1] CHENG DONG,[2] JEFFREY J. FREDBERG,[3] FARSHID GUILAK,[4] DONALD INGBER,[5] PAUL JANMEY,[1] ROGER D. KAMM,[6] GEERT W. SCHMID-SCHÖNBEIN,[7] and SHELDON WEINBAUM[8]

[1]University of Pennsylvania, Philadelphia, PA, USA; [2]Pennsylvania State University, University Park, PA, USA; [3]Harvard School of Public Health, Boston, MA, USA; [4]Duke University, Durham, NC, USA; [5]Harvard Medical School, Boston, MA, USA; [6]MIT, Boston, MA, USA; [7]University of California, San Diego, San Diego, CA, USA; and [8]City College of New York, New York, NY, USA

(Received 10 July 2008; accepted 21 February 2009; published online 4 March 2009)

Abstract—With the recent revolution in Molecular Biology and the deciphering of the Human Genome, understanding of the building blocks that comprise living systems has advanced rapidly. We have yet to understand, however, how the physical forces that animate life affect the synthesis, folding, assembly, and function of these molecular building blocks. We are equally uncertain as to how these building blocks interact dynamically to create coupled regulatory networks from which integrative biological behaviors emerge. Here we review recent advances in the field of biomechanics at the cellular and molecular levels, and set forth challenges confronting the field. Living systems work and move as multi-molecular collectives, and in order to understand key aspects of health and disease we must first be able to explain how physical forces and mechanical structures contribute to the active material properties of living cells and tissues, as well as how these forces impact information processing and cellular decision making. Such insights will no doubt inform basic biology and rational engineering of effective new approaches to clinical therapy.

Keywords—Biomechanics, Cell, Mechanics, Rheology, Signaling, Force, Stress.

emerge through collective interactions within dynamically coupled regulatory networks. Systems Biology presently emphasizes information transfer,[37] but the three-dimensional geometries and physical forces that play so large a role in biological structure and function have yet to be fully taken into account. Indeed, without these biomechanical factors there would be no form, no function, no life.

Most diseases present as a complex genetic profile with multiple changes in molecular expression.[85,131] Nonetheless, a patient goes to the doctor's office often because of a mechanical defect in a tissue or organ: a new swelling or lump, pain due to nerve compression, stiffness that limits movement, edema caused by a leak of tissue bodily fluids, constricted blood flow or lymph flow, or obstructed airflow that restricts breathing. Cures and remedies are often judged successful by the patient only when such mechanical defects are remedied. In order to understand health-related and disease-related aspects of living systems—all of which work and

Problem 3 - Cell mechanics research

The recent manuscript *"Biomechanics: Cell Research and Applications for the Next Decade"* by Discher, Dong, Fredberg, Guilak, Ingber, Janmey, Kamm, Schmid-Schönbein and Weinbaum discusses the challenges for cell mechanics now and in the future.

- Read the manuscript carefully and summarize it with approximately 150 words.
- The authors have identified ten major accomplishments in cell mechanics. List all the ten accomplishments by title.
- Select your favorite past accomplishment and describe it in less than 100 words.
- The authors have identified seven major challenges for the future. List all the seven future challenges by title.
- Select your favorite future challenge and describe it in less than 100 words.

Problem 4 - Final project

Inspired by the recent manuscript on major accomplishments and challenges in cell mechanics,

- Identify a title for your final project.
- Identify five key words for your final project.
- Write a tentative abstract of approximately 150-200 words.

Papers in the past have generally been about 4-6 pages long, two column, with about 3-5 figures and 8-12 references. Here are some examples of individual projects.

- Predicting microtubules structure using molecular dynamics
- The primary cilium: A well-designed fluid flow sensor
- The tensegrity paradigm
- Mechanotransduction in hair cells Translating sound waves into neural signals
- Modeling cell membrane dynamics
- Theoretical and experimental study of the penetration of the cell membrane
- Integrin and its role in mechanotransduction
- Finite element analysis of micropipette aspiration

the swimming velocity of mammalian sperm

Final Project ME239, Winter 2011

ME239 FINAL PROJECT

Sinusoidal model for flagellar motion

Sean Ramey
Department of Mechanical Engineering, Stanford University
Stanford, California

Abstract. Decreasing fertility and the rising fields of micro-fluidics and bio-mimicry have led to a more concentrated effort on studying the unique style of motility employed by sperm cells. Since the 1950's, the model developed by Hancock (1953) has been the leader in sperm modeling. This model is accurate but employs many complexities of fluid mechanics. Upon closer observation, the motion of the sperm's tail appears like that of a cork-screw and, when viewed from the side, behaves as a sinusoidal wave that propels the sperm by translating away from its body. When modeled as such, the absolute velocity of the sperm can be very accurately quantified for smaller sperm cells (0% error for human cells) and are within 20% for larger cells, such as those of the Chinese Golden Hamster. This simple model gives a easy and rapid way to quantify different characteristics of sperm cells and ultimately gives a more clear understanding of the methods through which sperm cells move.

MODELS AND MECHANISMS OF LEUKOCYTE EXTRAVASATION

Anusuya M. Ramasubramanian
Department of Biomechanical Engineering, Stanford University
Stanford, CA

ABSTRACT | Leukocyte extravasation is an innate immune system process by which white-blood cells leave the circulatory system and enter the inflamed tissue or site of infection.[1] Although leukocyte migration across the walls of microvessels was observed over 200 years ago, the molecular mechanisms of the migration were not clarified until the early part of the twentieth century.[2] Today, leukocyte extravasation is thought to occur in a multistep cascade involving the initial capture of the leukocyte by the endothelium, rolling of the leukocyte, slow rolling, arrest, adhesion and spreading of the white blood-cell, intraluminal crawling, and transmigration of the leukocyte across the endothelium.[1] Over the past two decades, a number of molecular and mechanical models have surfaced that view the leukocyte as a shell membrane, a hard sphere defined by Goldman hydrodynamics and liquid droplets. By exploring each leukocyte model in the context of the extravasation process, a greater insight into the importance of integrin and selectin-based mechanotransduction as well as the shear-flow-induced physics of extravasation can be gained. Such understanding can be particularly valuable in the context of drug and cancer development – two radically different processes that mimic leukocyte extravasation.

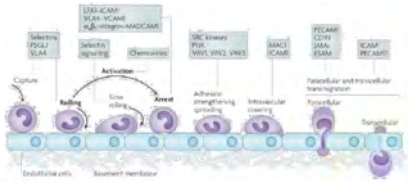

THE PRIMARY CILIUM: A WELL-DESIGNED FLUID FLOW SENSOR

Bryan C. Petzold
Department of Mechanical Engineering, Stanford University
Stanford, California

The primary cilium is a highly specialized surface projection which extends from the apical surface of almost every vertebrate cell. After its initial discovery over 100 years ago, primary cilia were long overlooked and even purported by some to be extraneous genetic remnants from our evolutionary past. However, in the past decade, a wealth of evidence has begun to accumulate, indicating that cilia in various cell types are not only as mechanical and chemical sensors, but also play important roles in intracellular signaling and cell division[2]. Some have even suggested that cilia-related dysfunction may have an important role in modern human epidemics such as obesity, hypertension and diabetes[3]. One such link between cilia-related dysfunction and human disease that has been explored extensively involves the role of the primary cilia of renal epithelial cells as flow sensors. It is believed that a dysfunction in these cilia results in polycystic kidney disease (PKD), the most common inherited disease in the United States, with an estimated 600,000 current cases[4]. Numerous models have been proposed to explain the mechanotransduction mechanism which allows the primary cilia of renal epithelial cells to detect fluid flow, but many questions remain. Understanding the transduction mechanism and the features of the primary cilium which make it an ideal flow sensor will not only answer many interesting questions in biology and biomechanics, but could aid in the treatment of PKD and other diseases which are caused by cilia-related dysfunction.

INTRODUCTION TO THE PRIMARY CILIUM

The primary cilium is a long, cylindrical, microtubule-based structure which extends from the apical surface of most vertebrate cells, as shown in Figure 1. In general, cells only have a single primary cilium. Referred to as the axoneme, the main structural element of the primary cilium is a collection of nine circumferentially-arranged doublet microtubules encased by membrane continuous with the cell membrane[1]. These doublet microtubules extend from a structure known as a basal body within the cell, which links the base of the primary cilium to the cytoskeleton. The basal body consists of nine triplet microtubules, and two of the microtubules of each triplet form the axoneme of the primary cilium[1]. Further structural support is provided by the transitional fibers (also shields), which add stability to the complex via attachment to the cell membrane[4]. In conjunction with a terminal plate at the end of the basal body, these transitional fibers also act as a protein fibril gate allowing certain proteins to enter and exit the cilium[5]. At the tip of the cilium, the axoneme becomes more variable, but is typically composed of nine single microtubules[1]. Although cilia are not isolated from the cell by a membrane, it seems reasonable to consider them to be organelles due to their unique structure, their extreme location past the cell periphery, and the selectivity to protein movement across their boundaries resulting from the transitional fibers and the terminal plate.

Depending on the species, primary cilia of renal epithelial cells typically vary between 2-20 μm in length *in vivo*[6]. However, lengths up to 30 μm have been observed *in vitro*[6]. In addition, studies involving mice renal epithelial cells measured primary cilia 2-3 μm long and 0.2 μm in diameter on average[7]. Since microtubules have an outer diameter of ~40 nm, this relatively small diameter indicates that nearly half the volume of a primary cilium is occupied by the microtubules alone[8].

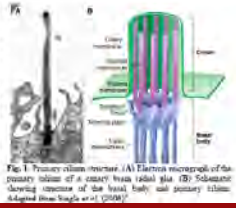

Fig. 1: Primary cilium structure. (A) Electron micrograph of the primary cilium of a canary brain tubal glia (B) Schematic drawing structure of the basal body and primary cilium. Adapted from Singla et al. (2006)[9].

Mechanisms of Neuron Repair and Stem Cell Neural Differentiation:

Neural Stem Cell Grafts and Current Advances in Spinal Cord Injury Research

Jeni Solimon

Abstract—Neural tissue regeneration and neuronal stem cell differentiation are discussed within the context of spinal cord injuries. The neuron is the fundamental element of the spinal cord and nervous system, and its functioning characteristics as well as the process of synaptic transmission are introduced to understand the impact of spinal cord injury. Three techniques are reviewed that address the issue of neural tissue regrowth from varying perspectives. The methods are introduced and demonstrate the potential role of neuron stem cell grafting in resolving severe spinal cord injury.

Index Terms—Neuron stem cell differentiation, axon ion discharge, synaptic transmission, spinal cord injury.

I. INTRODUCTION

SPINAL cord injuries represent a pervasive and often severe source of neurological trauma. The spinal cord represents the connection bridge between the central nervous system (CNS) and the peripheral nervous system (PNS). The CNS normally refers to the brain and spinal cord itself, where as the PNS is the vast network of nerves that permeates throughout the body. The human spinal cord consists of four main regions, as illustrated in Figure 1(a), each of which has a varying number of vertebrae, shown in Figure 1(b). The vertebrae have a set configuration network of nerves which then project, and thus the physiological impact of a spinal cord injury is directly correlated to the specific vertebrae effected.

Fig. 1. The spinal cord and the four primary vertebrae regions. (a)

Although there is a certain resilience in the specific effects of a spinal cord injury that stems from an individual's age and the nature of the impact, a general guideline can be arrived at that directly correlates the injured vertebrae with the most likely resulting region of sensory/mobility loss. Some specific conclusions are given in Table 1. As shown in the table, injuries in the cervical region normally tend to lead to major mechanical and sensory feedback loss, affecting a larger range of nerve networks than lower spinal regions since it is situated directly at the root of the brain-spinal cord interface. As the regions of spinal trauma moves further down the length of the spinal cord, the effected region is reduced in scope.

Spinal cord injuries themselves can be classified into two general categories: **complete** and **incomplete**. (9). In a **complete** injury, the damage is for the most part permanent and the effected individual usually exhibits little to no recovery of motor or sensory feedback. In **incomplete** injuries, the effects of the injury tend to be of a temporary nature and the individual may exhibit a full recovery. Two examples of individuals who experienced complete spinal cord injury are presented in Figure 2.

example: finite element simulation of pipette aspiration

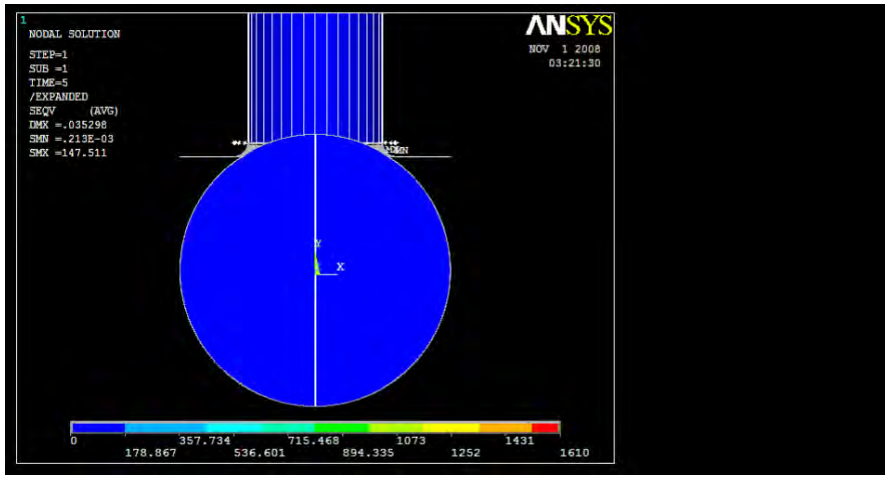

zubin huang [2007]

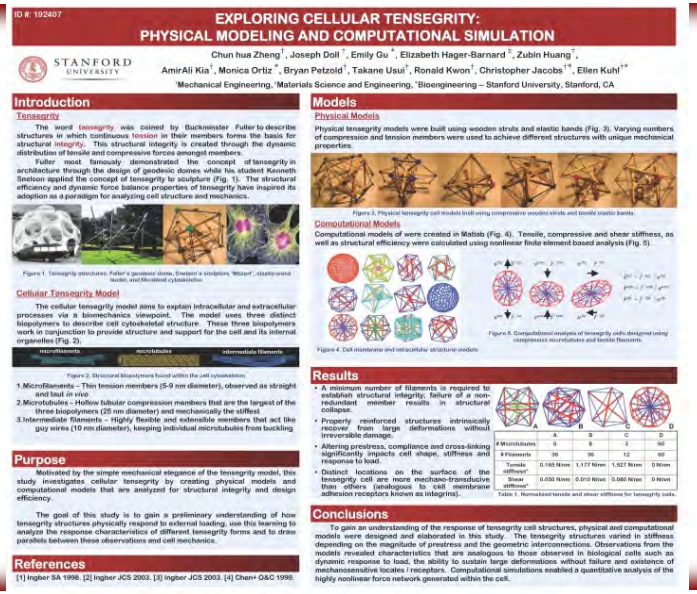

from molecular level to cellular level

assuming we know the mechanical properties of the individual filaments, what does that actually tell us about the assembly of filaments that we find in the cell?

- could we then predict the **stiffness of the overall assembly**?
- how does the filament microstructure affect **cytoskeletal properties**?
- how can we calculate the **macroscopic network properties** from the individual microscopic filament properties?

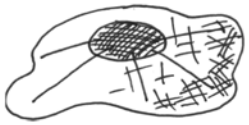

elements of the cytoskeleton
microtubules
intermediate filaments
actin filaments

Figure 4.1: The cytoskeleton provides structural stability and is responsible for forces during cell locomotion. Microtubules are thick hollow cylinders reaching out from the nucleus to the membrane, intermediate filaments can be found anywhere in the cytosol, and actin filaments are usually concentrated close to the cell membrane.

from molecular level to cellular level

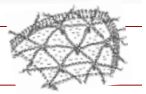

three examples

- **fiber bundle model** for filopodia
- **network model** for red blood cell membranes
- **tensegrity model** for generic cell structures

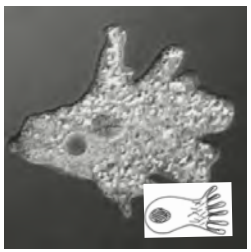

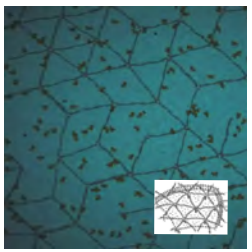

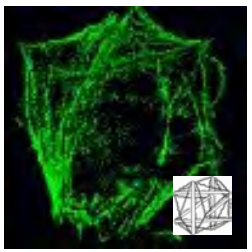

microstructural arrangement of actin

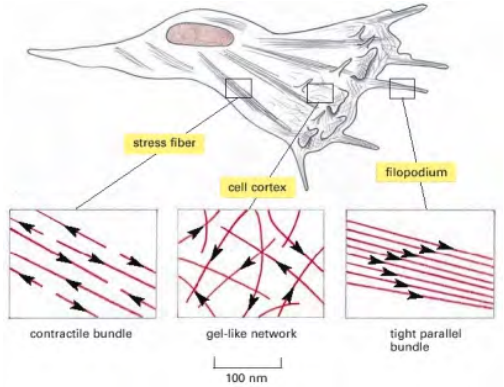

Figure 4.2.1. A crawling cell, drawn to scale, is shown with three areas enlarged to show the arrangement of actin filaments. The actin filaments are shown in red, with arrowheads pointing toward the plus end. Stress fibers are contractile and exert tension. The cell cortex underlies the plasma membrane. Filopodia are spike-like projections of the plasma membrane that allow a cell to explore its environments.

alberts, johnson, lewis, raff, roberts, walter [2002]

assembly of crosslinked actin filaments

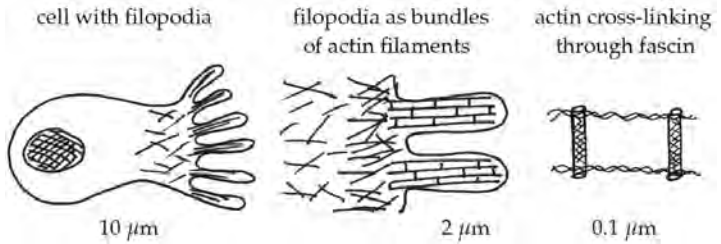

Figure 4.3. Bundles of actin filaments tightly crosslinked through fascin are known as filopodia. The mechanical properties of filopodia play an essential role in various different physiological processes including hearing, cell migration, and growth.

filopodia are very thin structures approximately 0.2 um in diameter. they can easily extend up to 2.0 um. they typically polymerize and depolymerize at rates of approximately 10 um/min. the mechanical properties of filopodia play an essential role in various different physiological processes, including hearing, cell migration, and growth. despite their importance to cell function, the structural architecture responsible for their overall mechanical behavior remains largely unknown.

pushing the envelope

simplified model for cell locomotion

- protrusion … polymerization at the leading edge of the cell
- attachment … formation of focal adhesions to link the cell to the surface
- retraction … contraction of stress fibers to retract the rear of the cell

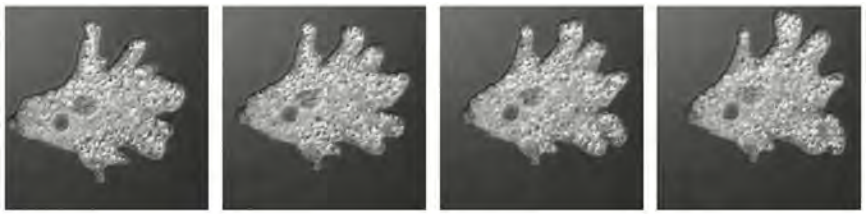

Figure 4.4: Single-celled amoeba crawling around by using actin polymerization to push out pseudopods to explore new territory. Organelles move in complex patterns within the cell,

alberts, johnson, lewis, raff, roberts, walter [2002]

pushing the envelope - critical length

Newton's third law: actio = reactio

$$F_{\text{fil}} \doteq F_{\text{mem}}$$

$$F_{\text{fil}} = \frac{\pi^2 EI}{[2L]^2} = \frac{\pi^2 EI}{4L} \qquad F_{\text{mem}} \approx 5\sqrt{n}\, r_{\text{act}}\, \text{pN/nm}$$

$$\frac{\pi^2 EI}{4L_{\text{crit}}^2} = 5\sqrt{n}\, r_{\text{act}} \frac{\text{pN}}{\text{nm}} \quad \text{thus} \quad L_{\text{crit}} = \frac{\pi}{2}\sqrt{\frac{EI}{5\sqrt{n}\, r_{\text{act}}\, \text{pN/nm}}}$$

$E = 1.9 \cdot 10^9$ N/m^2=1.9 GPa $\quad r_{\text{act}} = 3.5$ nm $\quad$ moment of inertia I

- loose assembly
- tightly crosslinked

case I - loosely assembled actin filaments

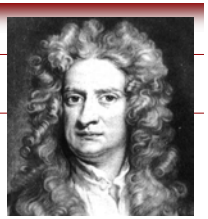

$$L_{\text{crit}} = \frac{\pi}{2}\sqrt{\frac{EI}{5\sqrt{n}\, r_{\text{act}}\, \text{pN/nm}}}$$

moment of inertia I

$$I = n\, I_{\text{act}} \qquad \text{with} \qquad I_{\text{act}} = \frac{\pi\, r_{\text{act}}^4}{4}$$

$$E = 1.9 \cdot 10^9\ \text{N/m}^2 = 1.9\ \text{GPa} \qquad r_{\text{act}} = 3.5\ \text{nm}$$

$$L_{\text{crit}} = \frac{\pi}{2}\sqrt{\frac{1.9 \cdot 10^9\,\text{N/m}^2 \cdot n\,\pi/4\,[3.5 \cdot 10^{-9}]^4\text{m}^4}{5\sqrt{n}\; 3.5 \cdot 10^{-12}\,\text{N}}} \approx 0.17769\,\mu\text{m}\; n^{1/4}$$

$$n = 30\ \text{filaments} \qquad L_{\text{crit}} = 0.416\,\mu\text{m}$$

much too low - disagrees with observations of 2um

case II - tightly crosslinked actin filaments

$$L_{\text{crit}} = \frac{\pi}{2}\sqrt{\frac{EI}{5\sqrt{n}\, r_{\text{act}}\, \text{pN/nm}}}$$

moment of inertia I

$$I = \frac{\pi\, r_{\text{fil}}^4}{4} = n^2\,\frac{\pi\, r_{\text{act}}^4}{4} \qquad \text{with } r_{\text{fil}} = \sqrt{n}\, r_{\text{act}}$$

$$E = 1.9 \cdot 10^9\ \text{N/m}^2 = 1.9\ \text{GPa} \qquad r_{\text{act}} = 3.5\ \text{nm}$$

$$L_{\text{crit}} = \frac{\pi}{2}\sqrt{\frac{1.9 \cdot 10^9\,\text{N/m}^2 \cdot n^2\,\pi/4\,[3.5 \cdot 10^{-9}]^4\text{m}^4}{5\sqrt{n}\; 3.5 \cdot 10^{-12}\,\text{N}}} \approx 0.17769\,\mu\text{m}\; n^{3/4}$$

$$n = 30\ \text{filaments} \qquad L_{\text{crit}} = 2.278\,\mu\text{m}$$

better model - agrees with observations of 2um

red blood cells

erythrocytes, red blood cells are essential to deliver oxygen to the body via the blood flow through the circulatory system. they take up oxygen in the lungs and release it while squeezing through the body's capillaries. adult humans have about 2-3 10^{13}, 20-30 trillion, red blood cells comprising about a quarter of the total amount of cells in the human body.

red blood cells

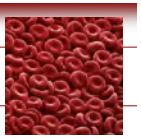

human mature red blood cells are **flexible biconcave disks** that lack a cell nucleus and most organelles. typical human erythrocytes have a disk diameter of 6–8µm, a thickness of 2µm, a volume of 90fL, and a surface of 136µm^2. they can swell to spherical shape of 150fL, without membrane distension. the membrane of the red blood cell plays a key role in regulating **surface deformability**, **flexibility**, and adhesion to other cells. these functions are highly dependent on its composition. the red blood cell membrane is composed of 3 layers: the glycocalyx on the exterior, which is rich in carbohydrates; the lipid bilayer consisting of lipidic main constituents and transmembrane proteins; and the membrane skeleton, a **structural network of proteins** located **on the inner surface** of the lipid bilayer.

red blood cells

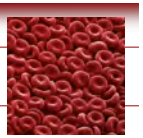

Metabolic remodeling of the human red blood cell membrane

YongKeun Park[a,b], Catherine A. Best[c], Thorsten Auth[d,e], Nir S. Gov[f], Samuel A. Safran[e], Gabriel Popescu[g], Subra Suresh[b,h,1], and Michael S. Feld[a,1]

[a]G. R. Harrison Spectroscopy Laboratory and [b]School of Engineering, Massachusetts Institute of Technology, Cambridge, MA 02139; [c]Harvard-Massachusetts Institute of Technology Division of Health Science and Technology, Massachusetts Institute of Technology, Cambridge, MA 02139; [d]College of Medicine and [e]Quantitative Light Imaging Laboratory, Department of Electrical and Computer Engineering, Beckman Institute for Advanced Science & Technology University of Illinois at Urbana-Champaign, Urbana, IL 61801; [f]Forschungszentrum Jülich, Institute for Solid State Research, 52425 Jülich, Germany; and [g]Department of Materials and Interfaces and [h]Department of Chemical Physics, Weizmann Institute of Science, P.O. Box. 26, Rehovot 76100, Israel

Edited by Zdeněk P. Bažant, Northwestern University, Evanston, IL, and approved November 25, 2009 (received for review September 18, 2009)

The remarkable deformability of the human red blood cell (RBC) results from the coupled dynamic response of the phospholipid bilayer and the spectrin molecular network. Here we present quantitative connections between spectrin morphology and membrane fluctuations of human RBCs by using dynamic full-field laser interferometry techniques. We present conclusive evidence that the presence of adenosine 5′-triphosphate (ATP) facilitates non-equilibrium dynamic fluctuations in the RBC membrane that are highly correlated with the biconcave shape of RBCs. Spatial analysis of the fluctuations reveals that these non-equilibrium membrane vibrations are enhanced at the scale of spectrin mesh size. Our results indicate that the dynamic remodeling of the coupled membranes powered by ATP results in non-equilibrium membrane fluctuations manifesting from both metabolic and thermal energies and also maintains the biconcave shape of RBCs.

red blood cells

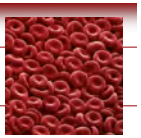

Metabolic remodeling of the human red blood cell membrane

YongKeun Park[a,b], Catherine A. Best[c], Thorsten Auth[d,e], Nir S. Gov[f], Samuel A. Safran[e], Gabriel Popescu[g], Subra Suresh[b,h,1], and Michael S. Feld[a,1]

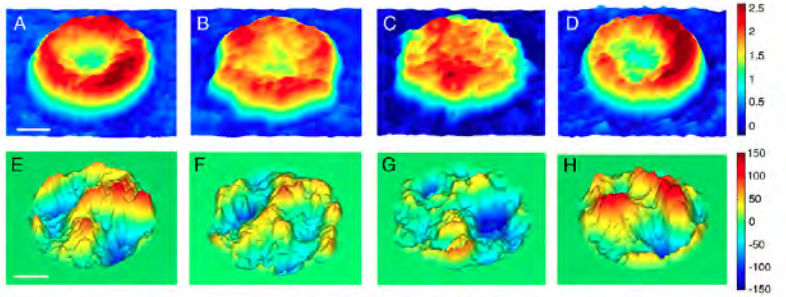

Fig. 1. Effects of ATP on morphology and dynamic fluctuation in RBC membrane. Topography of a healthy RBC, (*A*) of an ATP-depleted RBC (irreversible-ATP group), (*B*) of an ATP-depleted RBC (metabolic-ATP group), (*C*, and of a RBC with recovered ATP level (+ATP group), (*D*) resp. (*E–H*) Instantaneous displacement maps of membrane fluctuation in the Fig. 1*A–D*, resp. The scale bar is 2 μm. The colorbar scales are in μm and nm, resp.

red blood cells

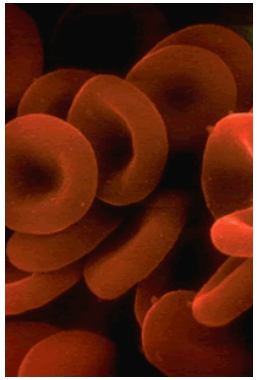

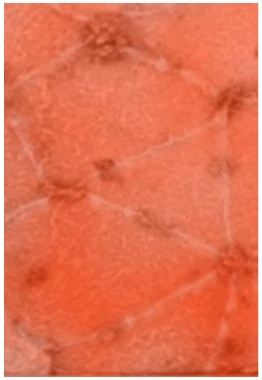

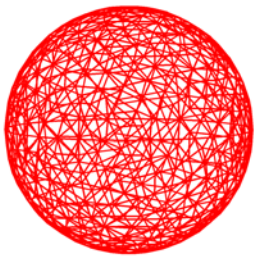

the human red blood cell membrane skeleton is a network of roughly 33,000 protein hexagons that looks like a microscopic geodesic dome

network model for red blood cells

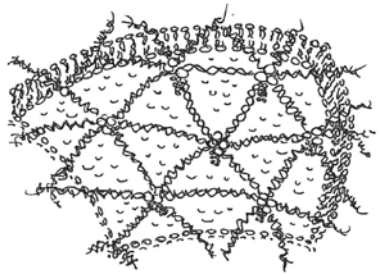

outer membrane surface
phospholipid bilayer
inner membrane surface

network of spectrin tetramers
crosslinked through actin

inner membrane surface

Figure 4.6: Microstructural architecture of the cell membrane of a red blood cell. A six-fold connected network of spectrin tetramers which are crosslinked through short actin filaments, anchored to the phospholipid bilayer, provides structural support to the inner cell membrane.

homogenization - hill-mandel condition

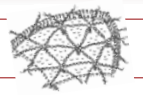

aim. to determine the overall material properties κ and μ of the network of spectrin chains in terms of the spectrin chain stiffness k

ENERGY APPROACH

$$W^{\text{mac}} \doteq W^{\text{mic}}$$

It has been shown how the central problem is reducible to the calculation of average stress or strain in one or other phase. A more versatile approach stems directly from classical theorems in elasticity and focusses attention on strain energies.

hill, r. elastic properties of reinforced solids: some theoretical principles, journal of the mechanics and physics of solids, 1963, 11:357–372.

different network kinematics

six-fold connected network

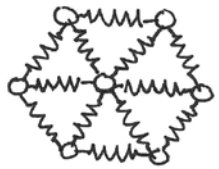

four-fold connected network

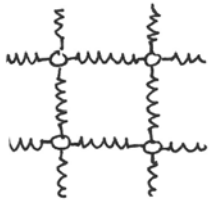

Figure 4.8: Microstructural architecture of a six-fold and four-fold connected network. The theory of homogenization helps to explain why nature prefers a six-fold connected network geometry.

single spring energy

free energy W^{spr} of a single spring

$$W^{\text{spr}} = \tfrac{1}{2}\, k\, \delta^2 = \tfrac{1}{2}\, k\, [\, l - l_0\,]^2 \qquad \text{where} \qquad \delta = l - l_0$$

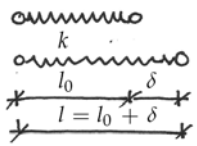

unstretched spring

stretched spring

k ... spring stiffness

Figure 4.7: Spectrin can be modeled as Gaussian chain which we can conceptually replace by an equivalent linear entropic spring with a spring stiffness of $k = 3\,\text{k}\,T\,N\,/\,L$. The strain energy of this spring can then be expressed as $W^{\text{spr}} = \frac{1}{2}\, k\, \delta^2$.

discrete microscopic network energy

extension

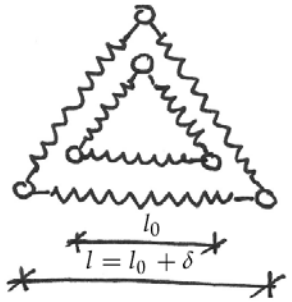

$$W^{\text{mic}} = \frac{\sum_{i=1}^{3} W_i^{\text{spr}}}{\sum_{i=1}^{3} A_i^{\text{spr}}}$$

$$\sum_{i=1}^{3} W_i^{\text{spr}} = 3\, W^{\text{spr}} = 3\, [\, \tfrac{1}{2}\, k\, \delta^2]$$

$$\sum_{i=1}^{3} A_i^{\text{spr}} = 3\, A^{\text{spr}} = \tfrac{1}{2}\, \sqrt{3}\, l_0^2$$

$$W^{\text{mic}} = \frac{3\, \frac{1}{2}\, k\, \delta^2}{\frac{1}{2}\, \sqrt{3}\, l_0^2} = \sqrt{3}\, k\, \left[\frac{\delta}{l_0}\right]^2$$

equivalent macroscopic energy

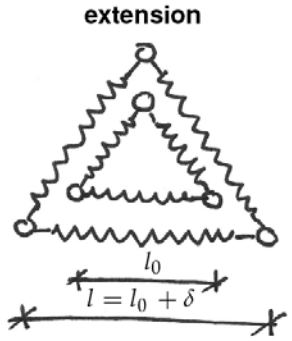

$$W^{\text{mac}} = \tfrac{1}{2}\kappa\,[\,\varepsilon_{xx} + \varepsilon_{yy}\,]^2 + \tfrac{1}{2}\mu\,[\,\varepsilon_{xx} - \varepsilon_{yy}\,]^2 + 2\,\mu\,\varepsilon_{xy}^2$$

micro-to-macro kinematics

$$\varepsilon_{xx} = \varepsilon_{yy} = \delta\,/\,l_0 \qquad \varepsilon_{xy} = 0$$

$$W^{\text{mac}} \doteq W^{\text{mic}}$$

$$\tfrac{1}{2}\kappa\left[\frac{\delta}{l_0} + \frac{\delta}{l_0}\right]^2 = \sqrt{3}k\left[\frac{\delta}{l_0}\right]^2$$

$$\underline{\underline{\kappa = \tfrac{1}{2}\sqrt{3}k}}$$

discrete microscopic network energy

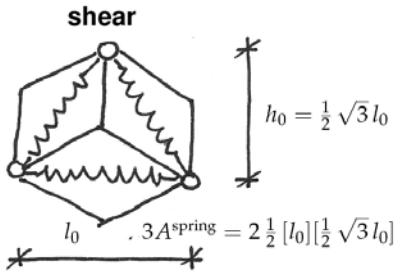

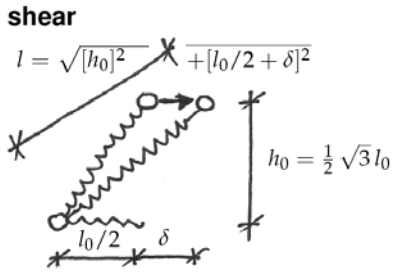

Figure 4.10: Illustration of representative area of three chains $3\,A^{\text{spring}} = \sqrt{3}/2\,l_0^2$ in six-fold connected network model, left. Illustatration of deformed spring length $l = l_0 + \delta/2$ in six-fold connected network model subjected to shear, right.

discrete microscopic network energy

shear

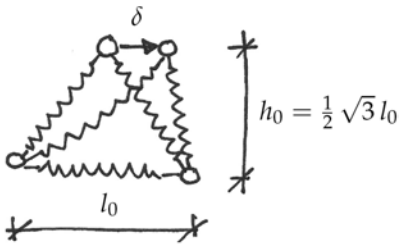

$$W^{\text{mic}} = \frac{\sum_{i=1}^{3} W_i^{\text{spr}}}{\sum_{i=1}^{3} A_i^{\text{spr}}}$$

$$\sum_{l=1}^{3} W_i^{\text{spr}} = \underbrace{\tfrac{1}{2}k\,[\,+\tfrac{1}{2}\delta\,]^2}_{\text{left spring}} + \underbrace{\tfrac{1}{2}k\,[\,-\tfrac{1}{2}\delta\,]^2}_{\text{right spring}} + \underbrace{0}_{\text{lower spring}} = \tfrac{1}{4}k\,\delta^2$$

$$\sum_{i=1}^{3} A_i^{\text{spr}} = 3\,A^{\text{spr}} = \tfrac{1}{2}\sqrt{3}\,l_0^2$$

$$W^{\text{mic}} = \frac{\frac{1}{4}k\,\delta^2}{\frac{1}{2}\sqrt{3}\,l_0^2} = \frac{\sqrt{3}}{6}k\left[\frac{\delta}{l_0}\right]^2$$

equivalent macroscopic energy

shear

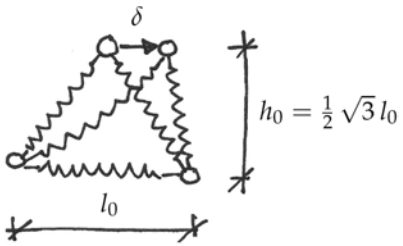

$$W^{\text{mac}} = \tfrac{1}{2}\kappa\,[\,\varepsilon_{xx} + \varepsilon_{yy}\,]^2 + \tfrac{1}{2}\mu\,[\,\varepsilon_{xx} - \varepsilon_{yy}\,]^2 + 2\,\mu\,\varepsilon_{xy}^2$$

micro-to-macro kinematics

$$\varepsilon_{xx} = 0 \qquad \varepsilon_{yy} = 0$$

$$\varepsilon_{xy} = \frac{1}{2}\left[\frac{\delta}{\frac{1}{2}\sqrt{3}\,l_0} + 0\right] = \frac{1}{\sqrt{3}}\frac{\delta}{l_0}$$

$$W^{\text{mac}} \doteq W^{\text{mic}}$$

$$2\,\mu\left[\frac{1}{\sqrt{3}}\frac{\delta}{l_0}\right]^2 = \frac{\sqrt{3}}{6}k\left[\frac{\delta}{l_0}\right]^2$$

$$\underline{\underline{\mu = \tfrac{1}{4}\sqrt{3}k}}$$